

光学学报

基于商用型空心阴极灯实现的法拉第反常色散原子滤光器

缑芝玉¹, 杨保东^{1,2,3*}, 赵韩帅¹, 周海涛¹

¹山西大学物理电子工程学院, 山西 太原 030006;

²山西大学量子光学与光量子器件国家重点实验室, 光电研究所, 山西 太原 030006;

³山西大学极端光学协同创新中心, 山西 太原 030006

摘要 基于铯原子 $6S_{1/2}$ - $6P_{3/2}$ 跃迁线, 在商用型空心阴极灯中, 实现了工作波长为 852 nm 的法拉第反常色散原子滤光器 (FADOF); 当铯空心阴极灯工作电流在 1~4 mA 范围内时, 可获得单峰、共振的线芯式 FADOF; 当铯空心阴极灯工作电流在 6~10 mA 范围内时, 可获得线翼式 FADOF。实验上系统测量了工作电流、轴向磁场强度、信号光功率对 FADOF 性能的影响, 优化参数下该滤光器的透射率高达 77%。

关键词 光学器件; 滤光器; 磁致旋光; 遥感; 空心阴极灯

中图分类号 O562

文献标志码 A

DOI: 10.3788/AOS221581

1 引言

法拉第反常色散原子滤光器 (FADOF) 因具有窄带宽、高透射率和高背景噪声抑制等优点, 已被广泛应用于自由空间光通信^[1-2]、雷达遥感系统^[3-4]和稳频激光系统^[5-6]等领域中。研究人员针对不同种类的原子, 基于原子基态-激发态的跃迁线对 FADOF 进行了理论和实验研究: 基于钠原子 $3S_{1/2}$ - $3P_{1/2}$ 跃迁线实现的工作波长为 589 nm 的 FADOF^[7]; 基于铷原子 $5S_{1/2}$ - $6P_{3/2}$ 、 $5S_{1/2}$ - $5P_{3/2}$ 、 $5S_{1/2}$ - $5P_{1/2}$ 跃迁线实现的波长为 420、780、795 nm 的 FADOF^[8-11]; 基于铯原子 $6S_{1/2}$ - $6P_{3/2}$ 、 $6S_{1/2}$ - $7P_{1/2}$ 、 $6S_{1/2}$ - $7P_{3/2}$ 跃迁线实现的波长为 852、459、455 nm 的 FADOF^[12-15]。这些工作^[7-15]系统地测量了轴向磁场大小、信号光功率大小、原子气室温度和缓冲气体种类对 FADOF 性能的影响。为了使 FADOF 工作波长有更多的选择性, 以适应更多领域的应用需求, 研究人员又开展了基于原子激发态-激发态跃迁线之间的滤光器 (ES-FADOF) 研究: 基于铷原子的激发态 $5P_{3/2}$ - $4D_{5/2}$ 跃迁线, 通过直接激光泵浦的方式实现了处于光通信波段的 1529 nm ES-FADOF^[16]; 基于铷原子的 $5P_{3/2}$ - $8D_{5/2}$ 跃迁线, 通过直接激光泵浦的方式实现了波长为 543 nm 的 ES-FADOF^[17]; 基于铯原子的激发态 $5D_{5/2}$ - $6F_{7/2}$ 跃迁线, 通过间接激光泵浦的方式实现了

728 nm ES-FADOF^[18]。ES-FADOF 与 FADOF 的不同点在于, 它一般需要通过泵浦光将原子由基态激发居到所需要的中间激发态上^[16-19]。

无论是 FADOF, 还是 ES-FADOF, 其实验构型一般都是一个信号光通过处于一对正交棱镜之间的原子介质。为了提高滤光器的透射率, 一方面需要沿信号光传播方向施加一定强度的磁场, 使线偏振信号光的偏振面发生旋转, 达到磁致旋光的目的。另一方面, 通常需要对原子气室加热控温, 以提高原子的数密度, 增强光与原子之间的相互作用, 从而增加滤光器的透射率。然而, 对于一些熔点较高的原子介质, 为了获得具有较高数密度的原子样品, 需要加热原子气室到足够高的温度, 这通常是不方便的。为此, 有些学者注意到常用于原子吸收光谱仪的锐线光源(空心阴极灯、无极灯等元素灯)都是通过原子之间的碰撞激发而发光的。原子在碰撞的过程中也提高了灯内原子样品的数密度。利用这一点, 研究人员基于特殊设计的铷原子无极灯实现了工作波长处于激发态 $5P_{3/2}$ - $5D_{5/2}$ 跃迁线之间的 776 nm ES-FADOF, 滤波器带宽约为 650 MHz^[20], 还实现了工作波长处于激发态 $5P_{3/2}$ - $4D_{5/2}$ 跃迁线之间的 1529 nm ES-FADOF^[21]。也有研究人员基于特殊设计的 see-through 型空心阴极灯, 利用其灯内高密度的原子样品开展一些光谱研究(饱和吸收

收稿日期: 2022-08-09; 修回日期: 2022-09-06; 录用日期: 2022-09-13; 网络首发日期: 2022-09-23

基金项目: 国家自然科学基金(61975102, 11974226)、国家重点研发计划(2017YFA0304502)、山西省自然科学基金(20210302123437)、山西省高等学校科技创新项目(2019L0101)

通信作者: *ybd@sxu.edu.cn

光谱^[22]、偏振光谱^[23]和调制转移光谱^[24]等),以及激光器的稳频^[25]和原子能级结构的测量^[26]等研究工作。

本文是基于商用型空心阴极灯(HCL),通过调节HCL的工作电流来控制灯内原子的数密度,基于铯原子的 $6S_{1/2}$ - $6P_{3/2}$ 跃迁线,实现了波长为852 nm的FADOF,该波长位于大气的一个透明窗口内,在自由空间激光通信中具有一定的应用价值。

2 实验原理及装置

图1为与实验相关的铯原子能级图。基态 $6S_{1/2}$ 有两个超精细能级 $F=3$ 和 $F=4$,之间的频率间隔为9192.6 MHz。激发态 $6P_{3/2}$ 有4个超精细子能级($F'=2$ 、 $F'=3$ 、 $F'=4$ 和 $F'=5$),之间的频率间隔分别为151.2、201.3、251.1 MHz。图2为实验装置示意图,其中QWP为1/4波片,M为反射镜。波长为852 nm的光

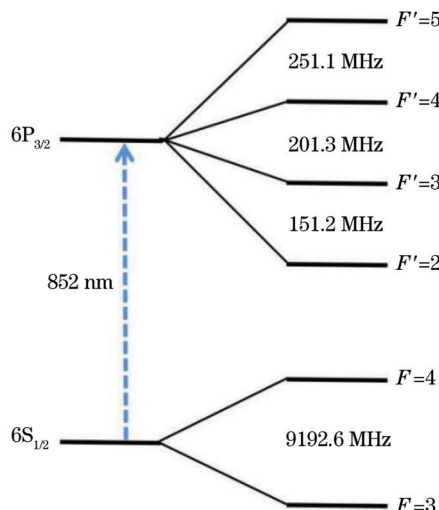


图1 与实验相关的铯原子能级图

Fig. 1 Energy level diagram of cesium atom relevant to experiment

栅外腔反馈半导体激光器(EDL)出射激光,将其频率调谐到铯原子的 $6S_{1/2}$ - $6P_{3/2}$ 跃迁线。852 nm激光束先经过光学隔离器(OI),然后经半波片(HWP)和立方偏振棱镜(PBS)分为两束:一束用于饱和吸收光谱(SAS)实验,在探测器PD1处获得光谱信号,作为频率参考;另一束作为FADOF实验中的信号光,通过处于一对正交的格兰-泰勒棱镜(G-T,其消光比为 $10^5:1$)之间的HCL,在探测器PD2处获得FADOF透射光谱信号。铯元素HCL内充有一定量的缓冲气体(氩气)与铯原子相互碰撞,导致铯原子激发和自发辐射发光。实验中灯体始终保持竖直,受HCL原理和构造的影响,灯体内不同位置处的铯原子分布并不均匀。通过多次实验,选择了信号光束通过灯体的最佳位置,即阳极和空心阴极之间的缝隙,该处灯体的直径约为3 cm,如图2所示。灯内铯原子数密度是通过调节HCL工作电流的大小来控制的,磁场是由一对沿厚度方向充磁的永磁环H1和H2(外径为33 mm、内径为22 mm、厚度为10 mm)提供,通过改变两磁环之间的距离来控制轴向磁场的大小。铯原子样品区域处,磁场的不均匀性小于10%,对FADOF实验的影响可以忽略。忽略实验系统的各种光损耗,FADOF透射率 T 的定义为两块格兰-泰勒棱镜偏振方向垂直时的透射激光功率与平行时的最大透射激光功率之比^[15]。理论上,透射率 T ^[3, 17]可以表示为

$$T = \frac{I_{\text{out}}}{I_{\text{in}}} = \frac{1}{4} \left\{ \exp[-\alpha_+(\omega)L] + \exp[-\alpha_-(\omega)L] - 2\cos[2\phi(\omega)] \exp\left[-\frac{\alpha_+(\omega) + \alpha_-(\omega)}{2}L\right] \right\}, \quad (1)$$

式中: I_{in} 和 I_{out} 为信号光入射和出射FADOF时的功率; α_+ 和 α_- 为线偏振信号光的左圆偏振组分和右圆偏振组分经过原子介质的吸收系数; L 为原子介质的长度; $\phi(\omega)$ 为法拉第旋转角。

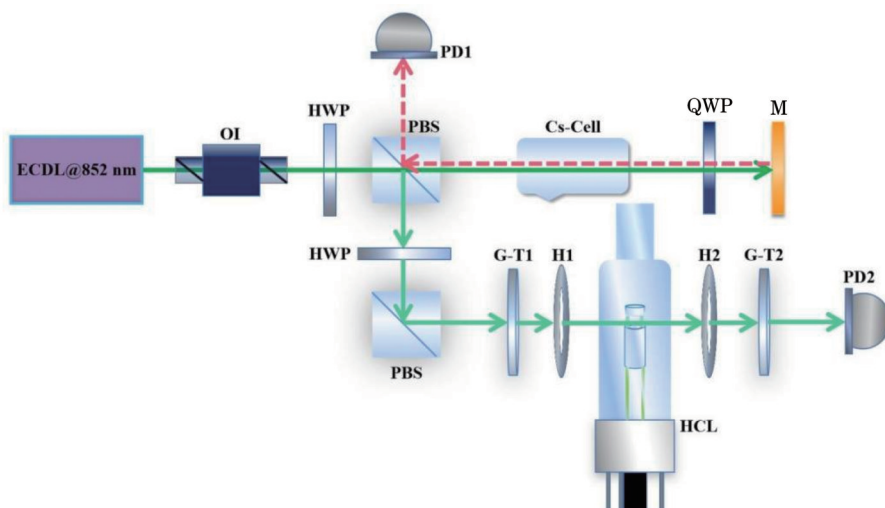


图2 基于商用型HCL的FADOF系统的实验装置示意图

Fig. 2 Experimental setup for FADOF system based on commercial-type HCL

3 实验结果及讨论

当852 nm信号光频率在铯原子 $6S_{1/2}(F=4)$ - $6P_{3/2}$ 跃迁线之间扫描,其功率为 $160 \mu\text{W}$,铯元素HCL的工作电流分别为2、4、6、8、10 mA时,信号光通过HCL内的铯原子介质(无磁场)后的吸收光谱如图3所示,SAS作为频率参考。可以清楚地看到,随着工作电流的增加,铯原子介质对信号光的吸收增强,表现为吸收光谱

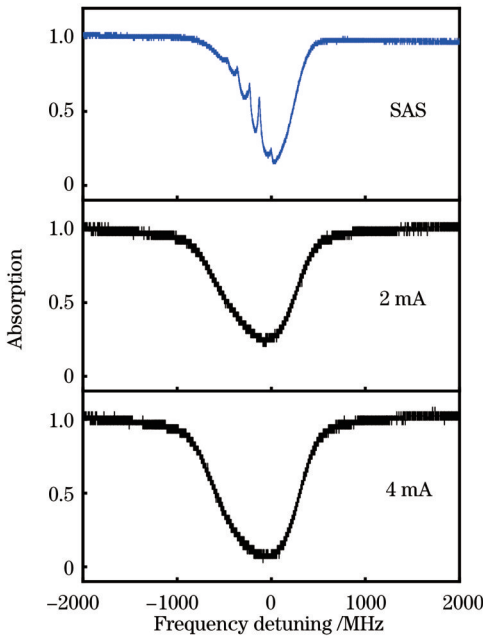


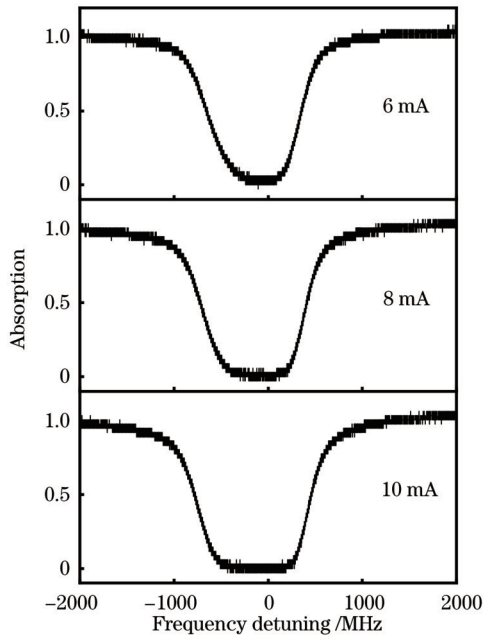
图3 不同工作电流下852 nm信号光通过铯HCL后的吸收光谱

Fig. 3 Absorption spectra of 852 nm signal light passing through cesium HCL under different working currents

当852 nm信号的光功率约为 $180 \mu\text{W}$,轴向磁场约为 $1.9 \times 10^{-2} \text{ T}$ 时,典型的FADOF光谱随铯元素HCL工作电流的演化如图4所示。当电流在1~4 mA之间时,滤光信号是单峰、共振的,属于典型的线芯式FADOF,可能是由HCL内充有一定量的缓冲气体造成的^[27]。当电流在6~10 mA之间时,透射的滤光信号呈双峰结构,位于铯原子共振吸收线的两侧,属于典型的线翼式FADOF。在与图4相同的实验参数下,FADOF的峰值透射率随HCL的工作电流和信号光功率的变化如图5(a)、(b)所示。随着工作电流的增加,HCL内铯原子数密度增加,磁致旋光效应必然增强,故FADOF的峰值透射率呈上升趋势。在固定的工作电流下,FADOF的峰值透射率随着信号光功率的增加整体呈下降趋势,在文献[28]中也有报道。在优化的实验参数下,当信号光功率约为 $130 \mu\text{W}$,轴向磁场约为 $1.9 \times 10^{-2} \text{ T}$,工作电流约为10 mA时,FADOF透射率高达77%。

入射852 nm信号光频率在铯原子 $6S_{1/2}(F=4)$ - $6P_{3/2}$ 跃迁线之间扫描,功率约为 $280 \mu\text{W}$,轴向磁场强度分别为 1.5×10^{-2} 、 1.8×10^{-2} 、 2.1×10^{-2} 、 2.4×10^{-2} 、 2.7×10^{-2} 、 $3.0 \times 10^{-2} \text{ T}$,FADOF光谱信号演

底部平坦的区域逐渐增宽,表明HCL内铯原子的数密度越来越高,而其灯体本身的温度较低。通常气室中的原子数密度提升是通过对气室加热来实现的,对熔点较高的元素就需要加热到足够高的温度来获得一定数密度的原子样品。然而,在FADOF实验中,还需要在气室周围放置永磁体来产生一个轴向均匀、稳定的磁场,过高的气室温度(大于居里温度)可能会影响到永磁体的性能,HCL的使用为解决该问题提供了一个途径。



化如图6所示。可以发现:当电流为4 mA时,光谱信号为线芯式FADOF信号^[15, 27];当电流为8 mA时,光谱信号为线翼式FADOF信号^[12-13]。FADOF信号峰值透射率随磁场的变化如图7所示。对于工作电流为4 mA的线芯式FADOF信号,当磁场强度从 $1.5 \times 10^{-2} \text{ T}$ 增加到 $3.0 \times 10^{-2} \text{ T}$ 时,法拉第磁致旋光效应增强,峰值透射率整体呈上升趋势。对于工作电流为8 mA的线翼式FADOF信号,当磁场强度在 1.5×10^{-2} ~ $2.1 \times 10^{-2} \text{ T}$ 范围内变化时,FADOF峰值透射率上升至最大值41.6%。同时,塞曼效应导致的原子能级移动会使FADOF的光谱透射带宽增加,且双峰之间的频率间隔也会相应增加。当磁场强度大于 $2.1 \times 10^{-2} \text{ T}$ 时,FADOF的光谱透射带宽会进一步增加,甚至向多峰结构的FADOF光谱信号转化,故峰值透射率整体呈下降趋势^[15]。

对于FADOF系统的实际应用来说,等效噪声带宽(ENBW)是一个重要的参数。当信号光的频率位于FADOF的某一透射峰时,其他透射峰就等效为背景光噪声通道,故ENBW越窄,接收系统的信噪比就越高。理论上,ENBW表示与FADOF谱线下方等面积、高度在最大透射率处时矩形的宽度,其计算公

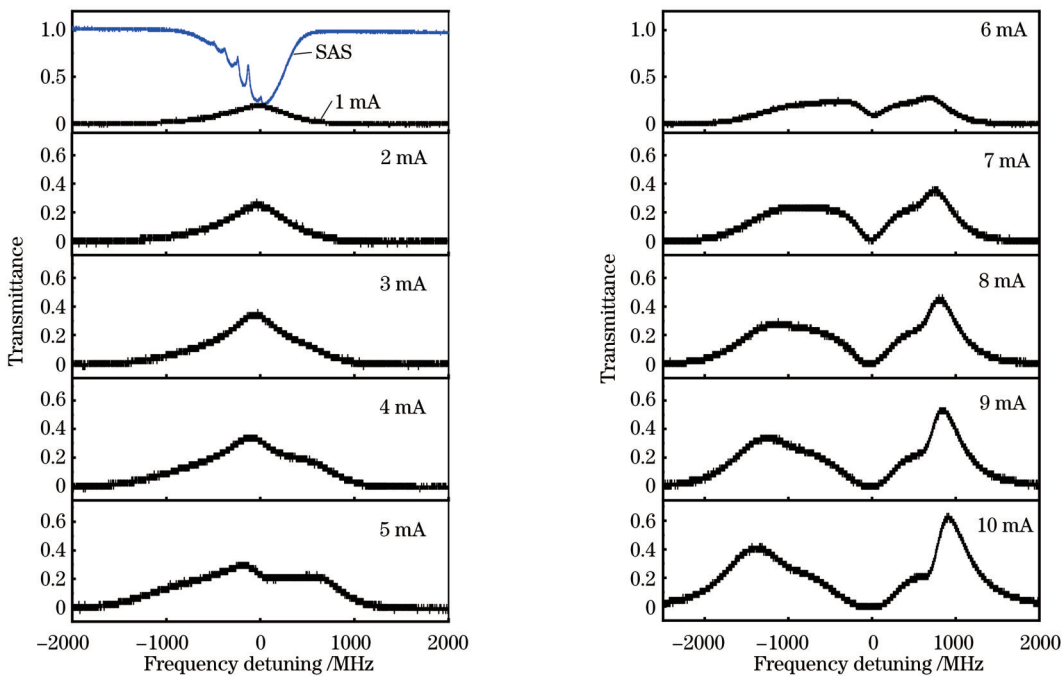


图4 FADOF透射谱随铯HCL工作电流的变化情况

Fig. 4 Transmittance spectrum of FADOF varying with working current of cesium HCL

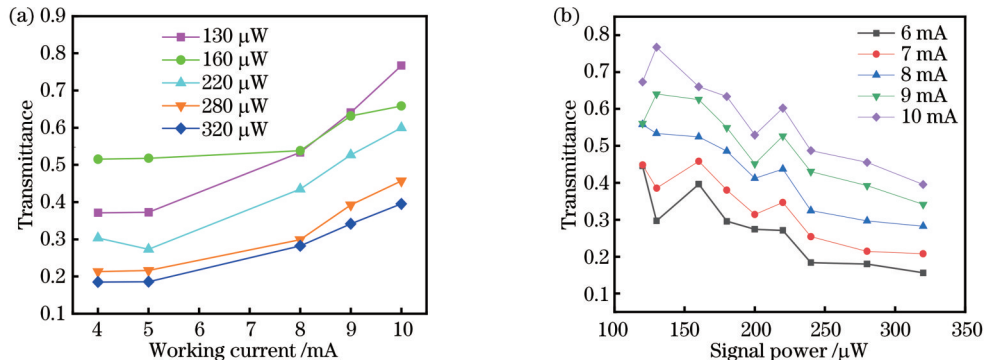


图5 FADOF的峰值透射率随铯HCL的工作电流和信号光功率的变化。(a)工作电流;(b)信号光功率

Fig. 5 Peak transmittance of FADOF varying with working current of cesium HCL and signal power. (a) Working current; (b) signal power

式^[14, 29]为

$$B_{\text{ENBW}} = \frac{\int_0^{\infty} S(v) dv}{S(v_m)}, \quad (2)$$

式中: $S(v)$ 为FADOF的透射率; v 为信号光的频率; v_m 为最大透射率处信号光的频率。在固定的信号光功率为 $280 \mu\text{W}$ 下,依据图6中的FADOF光谱实验数据,计算得到ENBW随轴向磁场强度的变化,如图8所示。可以发现,随着磁场强度的增加,ENBW大致呈上升趋势。通常在纯的铯原子介质中, $6S_{1/2}(F=4)$ - $6P_{3/2}$ 跃迁线处的FADOF光谱呈线翼式^[12-13]。然而,在本工作中,由于铯HCL内存在一定量的缓冲气体,故当工作电流为4 mA时,实验上获得了单峰、共振的线芯式FADOF信号,可被方便地用于法拉第稳频激光系统中^[6, 9]。当工作电流为8 mA时,可获得典型的

线翼式FADOF信号,透射光谱带宽较宽,如图6所示。以上区别导致HCL工作电流为8 mA时的ENBW(1.0~1.8 GHz)整体高于工作电流为4 mA时的ENBW(0.9~1.1 GHz),如图8所示。

4 结 论

基于铯原子 $6S_{1/2}(F=4)$ - $6P_{3/2}$ 跃迁线,实验上演示了利用商用型HCL实现FADOF,通过调节HCL工作电流的大小来控制灯内原子样品的数密度:当工作电流在1~4 mA范围内时,可获得单峰共振的线芯式FADOF;当工作电流在6~10 mA范围内时,可获得线翼式FADOF。这两种FADOF在稳频激光、雷达遥感等系统中有潜在的应用价值。在优化的实验参数下,FADOF的峰值透射率高达77%,ENBW小于1.8 GHz。铯原子本身的熔点较低($<28.5^\circ\text{C}$),故也

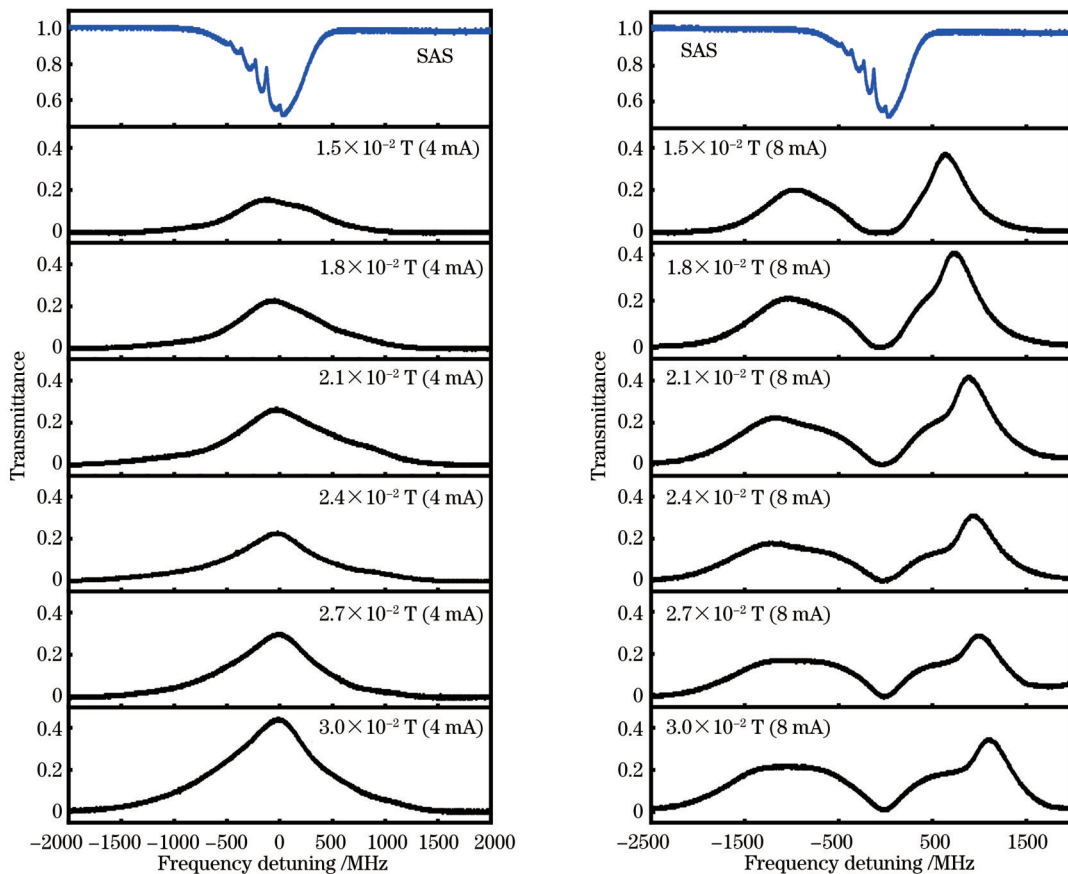


图 6 FADOF 透射光谱随轴向磁场的演变

Fig. 6 Transmittance spectrum of FADOF varying with axial magnetic field

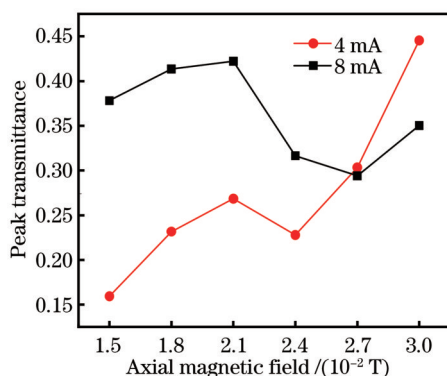


图 7 FADOF 峰值透射率随轴向磁场强度的变化

Fig. 7 Peak transmittance of FADOF varying with axial magnetic field

可在控温的铯原子气室中实现 FADOF。较低的温度也可获得具有较高数密度的原子样品,从而致使 FADOF 的透射率较高。显然,对于一些熔点较高的元素,基于商用型 HCL 实现 FADOF 将更有意义,特别是 HCL 在发光过程中,必然有部分原子已处于激发态。本研究成果为下一步尝试利用商用型 HCL 直接实现两个激发态跃迁线之间的 ES-FADOF 提供了参考。由于不再需要额外的泵浦激光将原子由基态布居到中间激发态,故本方案可达到简化同类实验装置、节约成本的目的。

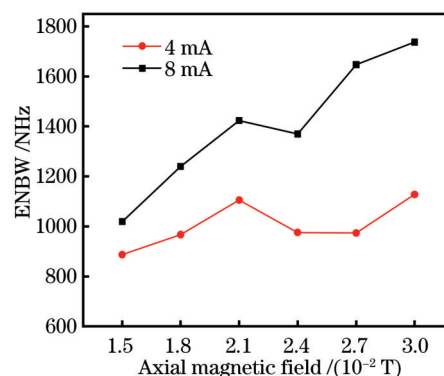


图 8 ENBW 随轴向磁场强度的变化

Fig. 8 ENBW varying with axial magnetic field

参 考 文 献

- [1] Chang P Y, Shi T T, Zhang S N, et al. Faraday laser at Rb 1529 nm transition for optical communication systems[J]. Chinese Optics Letters, 2017, 15(12): 121401.
- [2] Tang J X, Wang Q J, Li Y M, et al. Experimental study of a model digital space optical communication system with new quantum devices[J]. Applied Optics, 1995, 34(15): 2619-2622.
- [3] Popescu A, Walldorf D, Schorstein K, et al. On an excited state Faraday anomalous dispersion optical filter at moderate pump powers for a Brillouin-lidar receiver system[J]. Optics Communications, 2006, 264(2): 475-481.

- [4] Popescu A, Walther T. On an ESFADOF edge-filter for a range resolved Brillouin-lidar: the high vapor density and high pump intensity regime[J]. Applied Physics B, 2010, 98(4): 667-675.
- [5] Zhuang W, Chen J B. Active Faraday optical frequency standard [J]. Optics Letters, 2014, 39(21): 6339-6342.
- [6] Chang P Y, Chen Y L, Shang H S, et al. A Faraday laser operating on Cs 852 nm transition[J]. Applied Physics B, 2019, 125(12): 230.
- [7] Chen H, She C Y, Searcy P, et al. Sodium-vapor dispersive faraday filter[J]. Optics Letters, 1993, 18(12): 1019-1021.
- [8] Ling L, Bi G. Isotope ^{87}Rb Faraday anomalous dispersion optical filter at 420 nm[J]. Optics Letters, 2014, 39(11): 3324-3327.
- [9] Tao Z M, Hong Y L, Luo B, et al. Diode laser operating on an atomic transition limited by an isotope ^{87}Rb Faraday filter at 780 nm[J]. Optics Letters, 2015, 40(18): 4348-4351.
- [10] 郭弘, 党安红, 韩耀强, 等. Faraday反常色散滤光器[J]. 科学通报, 2010, 55(7): 527-533.
- Guo H, Dang A H, Han Y Q, et al. Faraday anomalous dispersion optical filter[J]. Chinese Science Bulletin, 2010, 55(7): 527-533.
- [11] Yan Y, Yuan J P, Wang L R, et al. A dual-wavelength bandpass Faraday anomalous dispersion optical filter operating on the D1 and D2 lines of rubidium[J]. Optics Communications, 2022, 509: 127855.
- [12] Zhang Y D, Jia X L, Bi Y, et al. Filter performance of a cesium Faraday optical filter at 852 nm[J]. Chinese Physics Letters, 2002, 19(6): 807-809.
- [13] Liu Y, Yang B D, Wang J M, et al. Demonstration of Faraday anomalous dispersion optical filter with reflection configuration [J]. Chinese Physics B, 2022, 31(1): 017804.
- [14] Xue X B, Pan D, Zhang X G, et al. Faraday anomalous dispersion optical filter at ^{133}Cs weak 459 nm transition[J]. Photonics Research, 2015, 3(5): 275-278.
- [15] Wang Y F, Zhang X G, Wang D Y, et al. Cs Faraday optical filter with a single transmission peak resonant with the atomic transition at 455 nm[J]. Optics Express, 2012, 20(23): 25817-25825.
- [16] Xiong J Y, Yin L F, Luo B, et al. Analysis of excited-state Faraday anomalous dispersion optical filter at 1529 nm[J]. Optics Express, 2016, 24(13): 14925-14933.
- [17] Rudolf A, Walther T. High-transmission excited-state Faraday anomalous dispersion optical filter edge filter based on a Halbach cylinder magnetic-field configuration[J]. Optics Letters, 2012,
- 37(21): 4477-4479.
- [18] Tao Z M, Zhang X G, Chen M, et al. Cs 728 nm excited state Faraday anomalous dispersion optical filter with indirect pump [J]. Physics Letters A, 2016, 380(25/26): 2150-2153.
- [19] 彭玉峰, 张文晋, 程祖海. 中间场下铷 532 nm 法拉第滤光器传输特性分析[J]. 光学学报, 2009, 29(7): 1778-1783.
- Peng Y F, Zhang W J, Cheng Z H. Analyses of transmission characteristics of rubidium Faraday optical filter at 532 nm in intermediate fields[J]. Acta Optica Sinica, 2009, 29(7): 1778-1783.
- [20] Sun Q Q, Zhuang W, Liu Z W, et al. Electrodeless-discharge-vapor-lamp-based Faraday anomalous-dispersion optical filter[J]. Optics Letters, 2011, 36(23): 4611-4613.
- [21] Sun Q Q, Hong Y L, Zhuang W, et al. Demonstration of an excited-state Faraday anomalous dispersion optical filter at 1529 nm by use of an electrodeless discharge rubidium vapor lamp[J]. Applied Physics Letters, 2012, 101(21): 211102.
- [22] Dammalapati U, Norris I, Riis E. Saturated absorption spectroscopy of calcium in a hollow-cathode lamp[J]. Journal of Physics B, 2009, 42(16): 165001.
- [23] Zhu S B, Chen T, Li X L, et al. Polarization spectroscopy of $^1\text{S}_0 - ^1\text{P}_1$ transition of neutral ytterbium isotopes in hollow cathode lamp[J]. Journal of the Optical Society of America B, 2014, 31(10): 2302-2309.
- [24] Wang W L, Xu X Y. Modulation transfer spectroscopy of ytterbium atoms in a hollow cathode lamp[J]. Chinese Physics Letters, 2011, 28(3): 033202.
- [25] Wang W L, Ye J, Jiang H L, et al. Frequency stabilization of a 399-nm laser by modulation transfer spectroscopy in an ytterbium hollow cathode lamp[J]. Chinese Physics B, 2011, 20(1): 013201.
- [26] Jang G H, Na M, Moon B, et al. Absolute frequency measurement of the $6s6p \ ^1\text{P}_1 - 6s7s \ ^1\text{S}_0$ transition of ^{174}Yb in a Yb hollow-cathode lamp[J]. Physical Review A, 2014, 89(6): 062510.
- [27] Xue X B, Tao Z M, Sun Q Q, et al. Faraday anomalous dispersion optical filter with a single transmission peak using a buffer-gas-filled rubidium cell[J]. Optics Letters, 2012, 37(12): 2274-2276.
- [28] Luo B, Yin L F, Xiong J Y, et al. Signal intensity influences on the atomic Faraday filter[J]. Optics Letters, 2018, 43(11): 2458-2461.
- [29] Bi G, Kang J, Fu J, et al. Ultra-narrow linewidth optical filter based on Faraday effect at isotope ^{87}Rb 420 nm transitions[J]. Physics Letters A, 2016, 380(47): 4022-4026.

Faraday Anomalous Dispersion Atomic Optical Filter Based on Commercial-Type Hollow Cathode Lamp

Gou Zhiyu¹, Yang Baodong^{1,2,3*}, Zhao Hanshuai¹, Zhou Haitao¹

¹College of Physics and Electronic Engineering, Shanxi University, Taiyuan 030006, Shanxi, China;

²State Key Laboratory of Quantum Optics and Quantum Optics Devices, Institute of Opto-Electronics, Shanxi University, Taiyuan 030006, Shanxi, China;

³Collaborative Innovation Center of Extreme Optics, Shanxi University, Taiyuan 030006, Shanxi, China

Abstract

Objective Faraday anomalous dispersion optical filter (FADOF) has many advantages such as narrow bandwidth, high transmittance, and excellent background rejection, and it has been widely used in optical communication, radar remote

sensing system, long-term frequency-stabilized laser system, and so on. In order to improve the transmittance of the optical filter, it is necessary to apply a certain intensity of magnetic field along the propagation direction of the signal light to rotate the polarization plane of the linearly polarized signal light according to the Faraday magneto-optic rotation effect. Besides, it is necessary to heat the temperature of the atomic vapor cell, so as to increase the number density of atoms, enhance the interaction between light and atoms, and thus improve the transmittance of a FADOF. However, for some atomic media with a high melting point, it is often inconvenient to heat the atomic vapor cell to a high enough temperature to obtain atomic samples with high number density. Some scholars have noticed that some light sources commonly used in atomic absorption spectrometers, such as hollow cathode lamps (HCLs) and electrodeless discharge vapor lamps, are excited by the collision between atoms. In the process of collision, the number density of the atomic samples in the lamp correspondingly increases. According to this point, we control the number density of atomic media in the lamp by adjusting the working current of the HCL and realize a FADOF with a wavelength of 852 nm based on the $6S_{1/2}-6P_{3/2}$ transition line of ^{133}Cs , and the wavelength is located in a transparent window of the atmosphere, which is helpful for free space laser communication.

Methods Experimental setup for the FADOF system based on the commercial-type HCL is shown in Fig. 2. The laser beam emitted from an external cavity diode laser (ECDL) at 852 nm with its frequency tuned to the $6S_{1/2}-6P_{3/2}$ transition line of ^{133}Cs first passes through an optical isolator (OI), and then is divided into two beams through a half-wave plate (HWP) and a polarizing beam splitter cube (PBS). Specifically, one beam is used for the saturated absorption spectrum experiment, and spectral signals are obtained at detector PD1 and taken as a frequency reference. The other beam is used as the signal light in the FADOF experiment, and a FADOF transmission spectral signal is obtained at the detector PD2 via a ^{133}Cs HCL located between a pair of orthogonal Glan-Taylor prisms. The number density of atoms in the HCL is controlled by adjusting the working current of the lamp. The magnetic field is provided by a pair of permanent magnet rings (H1 and H2), and the intensity of the axial magnetic field is controlled by changing the distance between the two magnetic rings.

Results and Discussions On the basis of $6S_{1/2}$ ($F=4$)- $6P_{3/2}$ transition line of ^{133}Cs , the FADOF is demonstrated using a commercial-type HCL in the experiment. The number density of the atomic sample can be changed by adjusting the working current of HCL (Fig. 3) instead of a temperature controller. Line-center FADOF with single-peak characteristic is realized in a working current of 1–4 mA due to the existence of buffer gas in HCL (Fig. 4). When the working current is 6–10 mA, the line-wing FADOF similar to popular FADOF in a ^{133}Cs vapor cell is also obtained (Fig. 4). These two kinds of FADOFs have potential applications in frequency stabilization laser and radar remote sensing systems. Under the optimized experimental parameters, the FADOF has a peak transmission rate of up to 77% and an equivalent noise bandwidth ENBW of less than 1.8 GHz (Fig. 8). In addition, a narrower ENBW usually indicates a stronger system ability to resist noise interference.

Conclusions A FADOF working in the line-center and line-wing operations at a particular working current is demonstrated in a commercial-type HCL based on the $6S_{1/2}-6P_{3/2}$ transition line of ^{133}Cs . The number density of the atomic samples in the lamp can be controlled by adjusting the working current of HCL. The ^{133}Cs atoms have a lower melting point (about 28.4 °C), and FADOF can be realized in the temperature-controlled vapor cell. Furthermore, higher atomic density can be obtained at a lower temperature, which results in a relatively high transmission of FADOF. Therefore, it is valuable to use the commercial-type HCL to realize FADOF based on the atom with a high melting point, and this HCL is expected to realize FADOF operating on the transition between two excited states for simplifying the experimental system, without an extra pumping laser.

Key words optical devices; optical filters; magnetic rotation; remote sensing; hollow-cathode lamp